Soft Matter

Accepted Manuscript

ROYAL SOCIETY OF CHEMISTRY

www.rsc.org/softmatter

Soft Matter

RSCPublishing

ARTICLE

Pairwise Interactions of Colloids in Two-dimensional Geometric Confinement

Cite this: DOI: 10.1039/x0xx00000x

Bum Jun Park*, Bomsock Lee, and Taekyung Yu*

Received 00th xxx xxx,
Accepted 00th xxx xxx

DOI: 10.1039/x0xx00000x

www.rsc.org/

We present the pairwise interaction behaviour of colloids confined in two-dimensional (2D) colloidal cages using optical laser tweezers. A single probe particle inside the hexagonal cage particles at a planar oil-water interface is allowed to diffuse freely and the spring constant is extracted from its trajectories. To evaluate the effect of multibody interactions, the pair interactions between the probe particle and each cage particle are directly measured by using optical tweezers. Based on pairwise additivity, Monte Carlo simulations are used to compare the values of the spring constant obtained from experiments and simulations. We find that the multibody interactions negligibly occur, and thus the particle interactions confined in such colloidal cages are highly pairwise. This work demonstrates that the use of the pairwise assumption in numerical simulations is rational when interparticle repulsive interactions are sufficiently strong, such as the particle interactions at fluid-fluid interfaces.

Introduction

Colloidal particles strongly and irreversibly adsorb to immiscible fluid-fluid interfaces.[1] The presence of solid particles leads to lower interfacial tension and subsequently stabilizes the interface, opening up important applications for conventional colloids as surface active additives.[2-5] Spherical polystyrene particles with surface functional groups, for example, exhibit abnormally strong and long-range repulsive interactions at an oil-water interface that are approximately hundreds of times larger than those in a single fluid phase (e.g., water).[6] The repulsive forces between two polystyrene particles at a decane-water interface were directly measured by using optical laser tweezers, and it was found that the force scales as $F \sim r^{-4}$, which is consistent with proposed models of electrostatic interactions.[6-13] The interaction magnitude is over a few piconewtons in separations (r) of several particle diameters. The repulsive interactions can be carefully tuned by adding electrolytes and/or surfactants in each fluid phase; these alter the Debye screening length and wettability of the particles at the interface.[14-16] The measured interaction forces of pairs at the oil-water interface are heterogeneous, so they directly relate to the bulk properties of 2D colloidal suspensions.[17]

The effect of multibody interactions may play a significant role in the microstructure and micromechanical properties of colloidal dispersions.[18, 19] A three-body interaction in an aqueous phase was previously measured to be attractive and was attributed to the overlap of double layers around the individual particles.[20] In the regimes involving strong repulsive interactions at fluid-fluid interfaces, however, neither multibody interactions nor pairwise additivity in the interaction potentials have been carefully studied yet. In this paper, in order to demonstrate whether the strong repulsive interactions at fluid-fluid interfaces are pairwise or not, we investigate the interaction behavior of a probe particle confined in hexagonal cage particles. The cage particles are held by optical laser tweezers and the single probe particle is allowed to diffuse freely inside the cage. Due to the strong electrostatic repulsions between the probe particle and the cage particles, we assume that the trajectories of the central probe particle can be determined by the pairwise potentials. We verify this pairwise additivity in multiparticle interactions by comparing experiments and Monte Carlo simulations. We also study the effect of interaction heterogeneity and thermal fluctuation of the cage particles on the probe particle motion.

Materials and Method

Materials

We use polystyrene particles (PS, Invitrogen Corporation) with a diameter of $2R \approx 3.0 \pm 0.2$ μm and a surface charge density of σ_s = 7.4 μC/cm^2. These particles are washed several times by repeated centrifugation and redispersion. The PS particles dispersed in water and isopropyl alcohol (IPA, Sigma-Aldrich) at 1:1 v/v are introduced to an oil-water interface in which IPA is used as a spreading solvent. The oil superphase is *n*-decane (Acros Organics, 99+%), which has been filtered through an aluminum oxide column (Acros Chemical, acidic activated, particle size 100-500 μm) to remove polar impurities. The

subphase is ultra-purified water (resistivity > 18.2 MΩ·cm) containing 0.1 mM sodium dodecylsulfate (SDS, Sigma-Aldrich).

The oil-water interface is formed in a fluid cell consisting of a glass outer cylinder and an inner cylinder made of aluminum and Teflon (Fig. 1).[14, 17] The outer cylinder is attached to a circular coverglass (No. 1.5 Fisher brand) using UV epoxy glue (Norland Products, NOA 81). Water passes through a gap provided by glass spacers such that the oil-water interface is pinned at the junction between the aluminum and Teflon of the inner cylinder at hydrodynamic equilibrium. The fluid cell is covered by another coverglass and sealed with vacuum grease to prevent evaporation and convection of the fluids. All glassware is treated by using a plasma cleaner (Harrick Plasma, PDC 32-G) to achieve a good wettability to water.

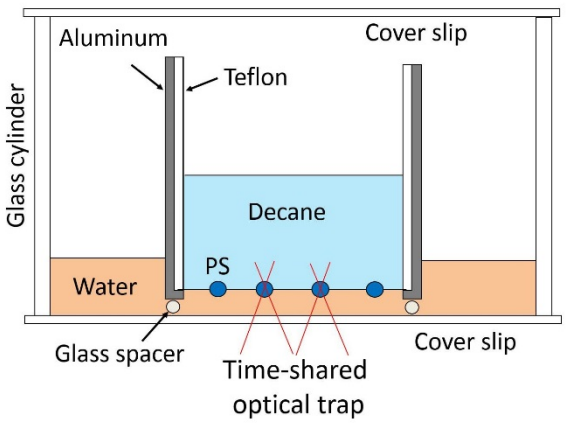

Fig. 1 Schematic of the flow cell.

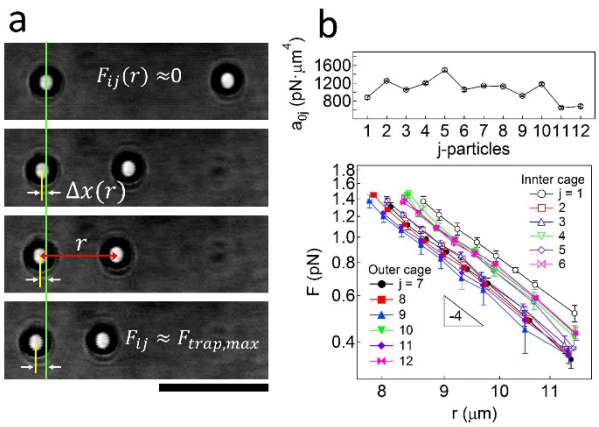

Fig. 2 Measurements of the pair interaction at the oil-water interface. (a) Snapshots of the pair interaction measurements. The scale bar is 10 μm. (b) The pair interaction forces of a probe particle (i = 0) with 12 particles (j = 1, 2,..., 12). The j particles form a single or a double hexagonal cage, and the probe particle is allowed to diffuse freely inside the cage. The magnitude of the interaction force, a_{0j}, fitted by using Eqs. 1 and 2, is shown at the top.

Pair Interactions

Time-shared optical tweezers are used to trap particles at the oil-water interface.[6, 21-23] To calibrate the optical trap stiffness ($\kappa_t = F_d/\Delta x$), a particle at the interface is held and subjected to Stokes drag forces by translating the motorized microscope stage at a constant velocity (u).[6, 24] Using the image analysis process,[21, 25, 26] the displacement of the particle (Δx) is measured as a function of the drag forces ($F_d = 6\pi R\eta_{eff}u$), where the effective viscosity can be approximated by using the relation, $\eta_{eff} = [\eta_o(1-\cos\theta_c) + \eta_w(1+\cos\theta_c)]/2$ where η_o and η_w are viscosities of oil and water, respectively.[6] The three-phase contact angle at the oil-water interface is approximately $\theta_c \approx 110°$ in the presence of 0.1mM SDS in the subphase.[27] Addition of SDS reduces the repulsive interactions between particles, enabling the particles to form a small colloidal cage without escaping from optical traps.[6, 14]

To measure the interaction force between two particles (i and j), particle i is held by a stationary trap and particle j approaches stepwise (Fig. 2a).[6] The particle displacement in the stationary trap from the equilibrium position (i.e., the green line in Fig. 2a) determines the pair interaction force using $F = \kappa_t\Delta x$, which is subsequently related to center-to-center separations (r_{ij}) between the two particles,

$$F_{ij} = \frac{A_{ij}}{r_{ij}^B} \quad (1)$$

where A_{ij} is the magnitude of the interaction force. The force measured by the optical tweezers (Eq. 1) is converted to potential energy based on the relation $F = -dU/dr$, $a_{ij} = A_{ij}/(B-1)$ and $b = B-1$,

$$\frac{U_{ij}}{k_BT} = \frac{a_{ij}}{r_{ij}^b} \quad (2)$$

where k_B is the Boltzmann's constant and T is the temperature. Note that upon measuring the pair interaction between the probe particle and a cage particle, the other ten particles trapped by optical traps are sufficiently separated from the pair (> 60μm). This experimental condition ensures that the other particles around the pair do not affect the pair interaction measurement.

To demonstrate that the optical trapping does not give rise to any artifacts in the particle interactions at the oil-water interface, we measured the pair interaction with varying the laser power and found that the laser power does not significantly affect the interaction magnitude. We also validated the pair interactions using passive measurements based on a particle trajectory analysis.[17] The resulting pair interaction force showed excellent agreement with that by the direct measurement of optical laser tweezers. Based on these experimental results, we believe that the interface strongly pins the particle surface, and thus, the three-phase contact angle is unlikely to change by the optical trapping. Moreover, based on a geometrical optics approximation in the optical trapping force calculations, we found that the radiation pressure normal to the interface in a typical tweezer experiment is not sufficient to

deform the interface and, consequently, the interface deformation-induced capillary interaction between particles is negligible.[22, 28]

Interactions in Colloidal Cages

To study the pairwise additivity in the interactions of a probe particle (i = 0) confined in colloidal cages, we organize j particles into a hexagonal cage composed of six particles (j = 1, 2,..., 6) held by stationary optical traps. The probe particle inside the cage is allowed to diffuse freely and to interact with the cage particles. We also use double cages with cobweb and honeycomb geometries consisting of twelve particles (j = 1, 2,..., 12).

Monte Carlo Simulations

Metropolis Monte Carlo (MC) simulation is compared with experimental results in terms of the interaction behaviour of a probe particle confined in colloidal cages. In the simulation, the cage particles (i.e., six particles for a single cage and twelve for a double cage) at the interface are fixed and a probe particle in the cage is allowed to diffuse freely. The probe particle interacts with its surrounding cage particles via electrostatic repulsive interactions (Eq. 2), where the magnitude of the interactions (a_{0j}) is obtained from the pair interaction measurements, as shown in Fig. 2b. Assuming pairwise additivity in the interactions, the total energy is the sum of the pair interactions (U_{0j} in Eq. 2) between the probe particle (i = 0) and the cage particles (j),

$$U_{pair} = \sum_j U_{0j} \ (j = 1\text{-}6 \text{ or } 1\text{-}12) \qquad (3)$$

We also study the effect of thermal fluctuation of the cage particles that are held in the trap potential,

$$U_{trap} = \frac{1}{2}\kappa_t \Delta\lambda^2 \qquad (4)$$

where $\Delta\lambda$ is the displacement from the equilibrium position of each cage particle trapped at stationary optical traps. In this case, the probe particle motion is determined by the total interaction, $U_{tot} = U_{pair} + U_{trap}$.

Results and Discussion

Optical laser tweezers are used to directly measure the pair interaction forces at an oil-water interface. As shown in Fig. 2b, the interaction force between the probe particle (i = 0) and each cage particle (j = 1, 2, 3,...) is found to be repulsive and shows the relation of $F \sim r^{-4}$ ($b = B - 1 \approx 3$). This scaling behaviour indicates that the repulsion is electrostatic in nature, consistent with previous studies.[6, 17] Notably, the broad distribution in measured forces in Fig. 2b implies interaction heterogeneity that can be attributed to non-uniform surface charge distribution,[17, 29, 30] but further quantitative studies are required to reveal the exact mechanism of the obtained interaction heterogeneity at the 2D colloidal system. Each force curve is fitted by using Eq. 1, and the interaction magnitude (a_{0j}) in Eq. 2 is shown at the top of Fig. 2b. The interaction magnitude averaged over twelve pairs is found to be $\langle a_{0j} \rangle$ = 1052 ± 28 pNμm^4 ($\langle a_{0j} \rangle / R^3 \approx 7.6 \times 10^4 k_B T$).

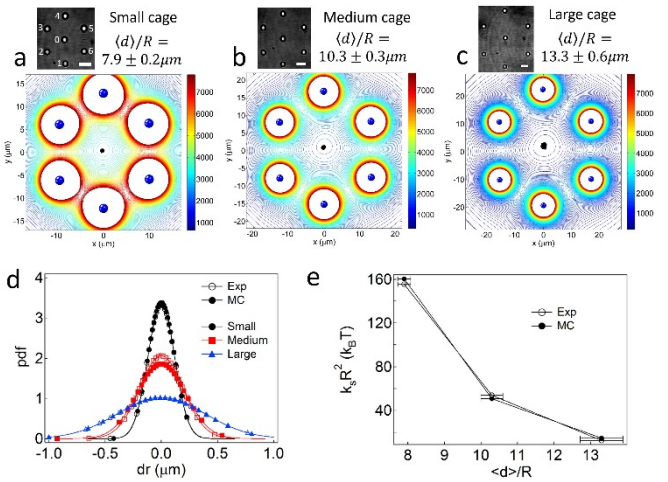

Fig. 3 Interactions in a single hexagonal cage. (a-c) Contour plots of the pairwise potential fields and experimental snapshots for three different cage size. The scale bar is 10 μm. (d) Comparison of probability density functions between the experiments and the MC simulations. (e) The corresponding spring constants depending on cage size.

To investigate the pairwise additivity in the interaction potential among multiple particles, we monitor the trajectories of the probe particle (i = 0) confined in hexagonal cage particles (j = 1-6 in Fig. 3) that are trapped by the stationary optical traps. The cage size is varied with a mean separation (or a lattice constant) between the cage particles normalized by the particle radius, $\langle d \rangle / R$ = 7.9 ± 0.2, 10.3 ± 0.3, and 13.3 ± 0.6. The contour plots in Fig. 3 indicate the potential fields determined by the pairwise additivity in the interactions between the probe particle and the cage particles (j = 1-6) in Fig. 2b. Blue dots in Fig. 3a-c indicate the cage particles. The potential field (contour lines) near each cage particle is not shown because the potential is extremely high compared to the region of interest around the probe particle (note that the electrostatic potential decays as $U \sim r^{-3}$). Black dots in the center region represent the experimental trajectories of the probe particle that are consistent with a location around the energy minimum as determined by the pairwise potential for all three cases with different cage sizes (Fig. 3a-c).

We compare the results of experiments and MC simulations based on the pairwise additivity in the interaction potentials (Eqs. 2 and 3). From the trajectories of the probe particle, the

displacements (dr) from the mean position are calculated. The corresponding probability density function (pdf) of a normal distribution ($\langle dr \rangle = 0$) is given by

$$f(dr|\langle dr\rangle, \sigma) = \frac{1}{\sigma\sqrt{2\pi}} e^{\frac{-(dr-\langle dr\rangle)^2}{2\sigma^2}} \quad (5)$$

where σ is the standard deviation. As shown in Fig. 3d, the pdf broadens as the cage size increases, indicating that the probe particle experiences a weaker repulsive potential as the cage size increases. The spring constant (k_s) is extracted using,

$$f(dr) = Ae^{\frac{-k_s dr^2}{2k_B T}} \quad (6)$$

where $k_s = k_B T/\sigma^2$. Fig. 3e shows the values of $k_s R^2$ obtained from the experiments and the simulations as a function of the cage size, $\langle d \rangle/R$. Both results are consistent with each other, suggesting that the probe particle motion is determined by the mean potential of the pairwise interactions.

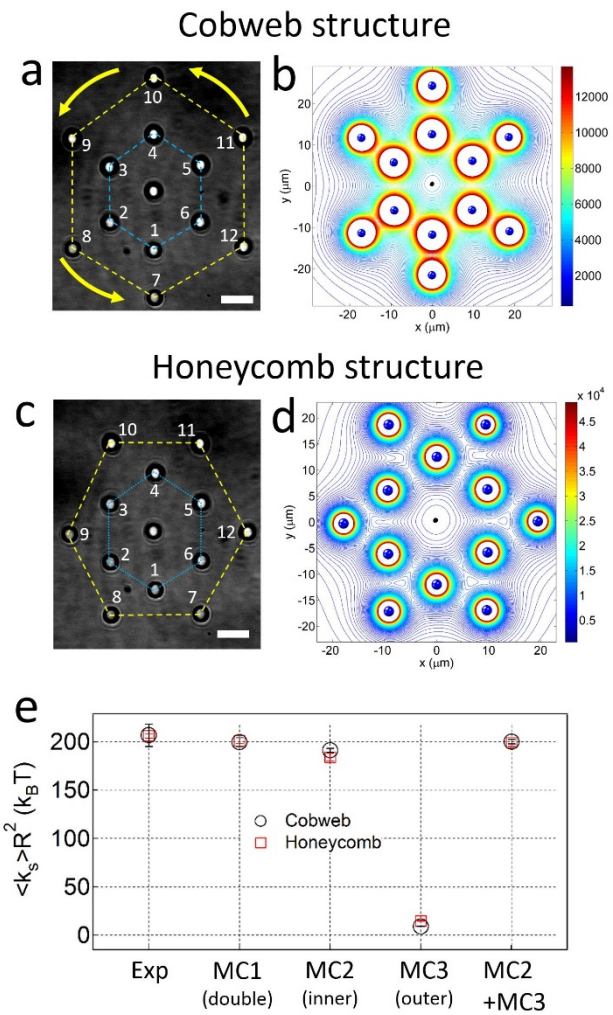

Fig. 4 Interactions in double cages: cobweb and honeycomb structures. (a, c) Experimental snapshots and (b, d) the corresponding contour plots of the pairwise potential fields of each cage structure. The scale bar is 10 μm. (e) Comparison of spring constants between experiments and MC simulations averaged over the rotational angle of the outer cage.

To further confirm the pairwise additivity in more complex geometries, we organize two cages with cobweb and honeycomb structures. These double cage structures can provide a clue as to how colloidal particles interact with each other across other particles. As shown in Fig. 4, the cobweb structure is the case when the individual particles composed of the two cages are aligned along with the probe particle. In the honeycomb structure, each outer cage particle is located between two particles in the inner cage such that the probe particle directly faces the outer cage particles.

The interaction of the probe particle with the double cage particles is also found to be pairwise. A hexagonal cage with a mean separation of $\langle d \rangle/R = 7.7 \pm 0.2$ is placed where it is surrounded by another hexagonal cage with $\langle d \rangle/R = 14.5 \pm 0.7$. The inner cage is fixed and the outer cage rotates in a counter clock-wise manner such that the structure switches from a cobweb to a honeycomb geometry, as shown in Fig. 4a and c, respectively. The trajectories of the free probe particle are monitored to extract the spring constant using Eqs. 4 and 5, while both inner and outer cages are held by the stationary optical traps. The pairwise potential field between the probe particle and the twelve cage particles based on the measured pair interactions (Fig. 2b) is shown in Fig. 4b for the cobweb and Fig. 4c for the honeycomb. Similar to the case of the single cage, it is observed that the experimental trajectories (black dots) of the probe particle are consistent with those determined by the energy minimum of the pairwise interaction potential.

To quantitatively investigate the effect of each cage, we perform MC simulations in the presence of the inner cage only (MC2), the outer cage only (MC3), and the double cage (MC1). The spring constant ($\langle k_s \rangle R^2$) averaged over the rotational angles of the outer cage (0 - 2π) in Fig. 4e indicates that the experimental result is in good agreement with the value of $\langle k_{s,MC1} \rangle R^2$ for both the cobweb and honeycomb geometries. The sum of the spring constants obtained from MC2 and MC3, $\langle k_{s,MC2} \rangle R^2 + \langle k_{s,MC3} \rangle R^2$, is also consistent with the $\langle k_{s,MC1} \rangle R^2$ and, thus, $\langle k_{s,MC1} \rangle = \langle k_{s,MC2} \rangle + \langle k_{s,MC3} \rangle$. These results confirm that the presence of the outer cage particles also influences the probe particle behaviour in the pairwise manner. Moreover, the negligible difference in the spring constants between the cobweb and honeycomb geometries suggests that the separations between the particles provide a major contribution for determining the behaviour of the probe particles confined in such colloidal cages. The results of the double cage system are eventually important in various numerical simulations for determining cut-off separations beyond which the interactions can be treated to be negligible, and therefore, computation time can be improved.

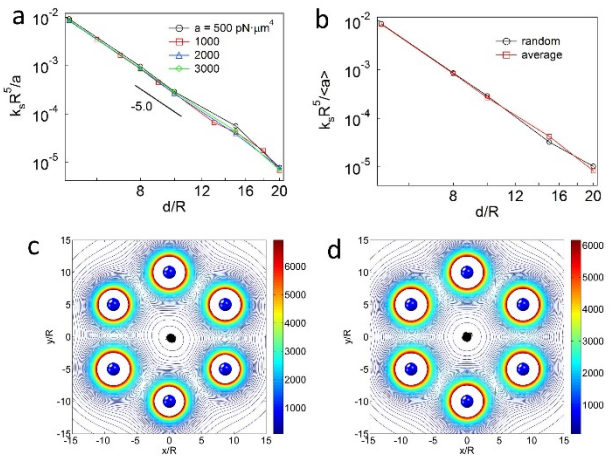

Fig. 5 The effect of the pair interaction magnitude on the spring constant in the single hexagonal cages using MC simulations. (a) The spring constant normalized by the particle size (R) and the magnitude of the homogenous pair interaction (a). (b) Comparison of the spring constants when random values of a_{0j} and the corresponding average value (a = <a_{0j}>) are used in the simulations. (c-d) Pairwise potential fields with (c) the random values of a_{0j} and (d) the average value (a = <a_{0j}>). The lattice constant is d/R = 10.

We use MC simulations to further investigate the relation between the spring constant and the pairwise interaction potential in a single hexagonal cage. It is found that the normalized spring constant (k_s) proportionally increases as the magnitude of homogenous pair interactions ($a = a_{0j}$) increases. The value of k_s is extracted from each run of MC simulation with varying the values of a and d, and is normalized by R and a. As shown in Fig. 5a, the normalized spring constant (k_sR^5/a) as a function of the normalized lattice constant (d/R) is consistent for the different values of a. The obtained power law exponent and the y-intercept in the logarithmic scale are found to be ~ -5.0 ± 0.03 and 1.47 ± 0.02, respectively. Therefore, a relation of the spring constant that describes a probe particle behaviour confined in single hexagonal cages is found to be,

$$\frac{k_sR^5}{a} \approx 30\left(\frac{d}{R}\right)^{-5}. \qquad (7)$$

This scaling behaviour suggests that the particle interaction in the symmetrically confined geometry can be dominantly determined by the lattice constant and the pairwise potential.

The probe particle in the single cages experiences a mean potential (a = <a_{0j}>) determined by the pairwise interactions when the pair interactions are heterogeneous (a_{0j}). In MC simulations, the values of a_{0j} are randomly generated in the range between 900 and 1500 pN·μm^4, which approximately corresponds to the range of the interaction magnitude for j = 1 - 6 particles in Fig. 2b. The mean value of the measured pair potentials, a = <a_{0j}> = 1268 pN·μm^4, is also used for comparison in MC simulations. As shown in Fig. 5b, the normalized spring constants in both cases of the heterogeneous and homogeneous potentials show good agreement with each other and with the results in Fig. 5a. Therefore, Eq. 7 can be generalized for the case when the interparticle interactions are heterogeneous. It is interesting to note that the interaction heterogeneity among particle pairs significantly affects the microstructure of a bulk suspension,[17] whereas the individual particles consisting of a unit hexagonal geometry experience the potential of mean force in the system.

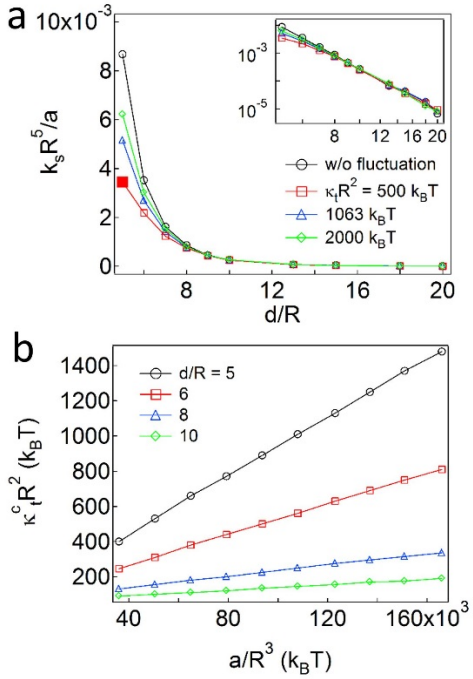

Fig. 6 The fluctuation effect of the single cage particles on the spring constant using MC simulations. The homogenous pairwise interaction potential (a) is used in the simulation. (a) The comparison of the spring constant with and without considering the thermal fluctuation of the cage particles, held by the optical traps. (b) The critical trap stiffness (κ_t^c) depending on the cage size and the interaction magnitude.

In experiments, the cage particles held by the stationary traps thermally fluctuate within the potential defined by the trap constant, κ_t. We examine this thermal fluctuation effect of the cage particles on the spring constant extracted from the probe particle motion using MC simulations. Similar to the experimental conditions, in the simulations, a particle located in a hexagonal cage is allowed to diffuse freely with a homogenous pairwise potential, $a = a_{0j}$ = 1000 pN·μm^4 ($a/R^3 \approx 7.2 \times 10^4\, k_BT$). The six cage particles are confined in the trap potential (Eq. 4), which should be much larger than 1 k_BT to trap them successfully. We use three different values of the trap stiffness, κ_tR^2 = 500, 1063, and 2000 k_BT, in which the value of 1063 k_BT corresponds to the experimental condition. As shown in Fig. 6a, for small size cages (i.e., d/R < 8), the extracted spring constant decreases as the value of κ_tR^2 decreases (Note that the case without the fluctuation represents $\kappa_tR^2 \to \infty$) . However, it is found that the thermal fluctuation negligibly affects the spring constant for large cages with $d/R \geq 8$ that we use in the experiments.

A particle held by the optical trap can escape from the trap when the displacement is larger than the half radius of the particle ($\Delta\lambda > R/2$).[31] The red filled square at $\kappa_t R^2 = 500\ k_B T$ in Fig. 6a indicates that the repulsive pair interaction (U_{0j}) overcomes the trap potential of the cage particles (U_{trap}), such that at least one of the cage particles should escape from the stationary trap. We define the critical value of the trap stiffness (κ_t^c) above which all cage particles stay at the stationary traps without being released from the optical traps. As shown in Fig. 6b, the value of κ_t^c linearly increases with the magnitude of the pair interaction potential (a). It is also found that κ_t^c quickly decays with the value of a as the cage size increases.

Conclusions

In summary, we have studied the interaction behaviour of a probe particle confined in colloidal cages held by the optical traps. The probe particle is allowed to diffuse freely inside the cage. We compare the experimental results with Monte Carlo simulations based on the pairwise additivity in the interaction potentials. We find that the position of the probe particle observed in experiments is consistent with the energy minimum determined by the pairwise interaction potentials. The spring constant is extracted from the trajectories of the probe particle in experiments and also shows excellent agreement with the simulation results. This consistency suggests that the interaction is highly pairwise and multibody interactions are negligible in such two-dimensional colloid systems in which the strong and long-range repulsive interactions are dominant. Based on the pairwise additivity in MC simulations, we also find that the probe particle experiences the mean potential averaged over the heterogeneous interactions between the probe particle and the cage particles. The importance in this work is to justify the use of the pairwise assumption in numerical simulations when interparticle repulsive interactions are sufficiently strong, such as the interactions between colloidal particles trapped at fluid-fluid interfaces. In this regard, we notice that the magnitude of the electrostatic repulsions at 2D colloidal systems can characterize a critical separation between particles beyond which the pairwise additivity becomes effective. This work therefore prompts further experimental and simulations studies to determine such critical separations in various systems by controlling interaction strength by using particles with different surface charges or altering electrolyte concentrations and wettabilities of particles at the interfaces.

Acknowledgements

B. J. Park acknowledges financial support from Basic Science Research Program through the National Research Foundation of Korea (NRF) funded by the Ministry of Science, ICT & Future Planning (NRF-2014R1A1A1005727) and a grant from Kyung Hee University in 2014 (KHU-20140324). T. Yu acknowledges funding from the Engineering Research Center of Excellence Program of Korea Ministry of Science, ICT & Future Planning (MSIP)/National Research Foundation of Korea (NRF-2014-009799). We thank Prof. E. M. Furst for the use of optical laser tweezers and Prof. J. Vermant for suggesting the particle geometries in experiments.

Notes and references

Department of Chemical Engineering, Kyung Hee University, Yongin, 446-701, South Korea

Corresponding authors:

Bum Jun Park: (Tel) +82-31-201-2429, (email) bjpark@khu.ac.kr

Taekyung Yu: (Tel) +82-31-201-2064, (email) tkyu@khu.ac.kr

1. B. P. Binks and T. S. Horozov, *Colloidal Particles at Liquid Interfaces*, Cambridge University Press, New York, 2006.
2. B. P. Binks, *Curr. Opin. Colloid Interface Sci.*, 2002, **7**, 21-41.
3. S. U. Pickering, *J. Chem. Soc. Trans.*, 1907, **91**, 2001-2021.
4. W. Ramsden, *Proc. R. Soc. London*, 1903, **72**, 156-164.
5. J.-W. Kim, D. Lee, H. C. Shum and D. A. Weitz, *Adv. Mater.*, 2008, **20**, 3239-3243.
6. B. J. Park, J. P. Pantina, E. M. Furst, M. Oettel, S. Reynaert and J. Vermant, *Langmuir*, 2008, **24**, 1686-1694.
7. A. J. Hurd, *J. Phys. A: Math. Gen.*, 1985, **45**, L1055-L1060.
8. K. Masschaele, B. J. Park, E. M. Furst, J. Fransaer and J. Vermant, *Phys. Rev. Lett.*, 2010, **105**, 048303.
9. M. Oettel and S. Dietrich, *Langmuir*, 2008, **24**, 1425.
10. P. Pieranski, *Phys. Rev. Lett.*, 1980, **45**, 569-572.
11. R. Aveyard, B. P. Binks, J. H. Clint, P. D. I. Fletcher, T. S. Horozov, B. Neumann, V. N. Paunov, J. Annesley, S. W. Botchway, D. Nees, A. W. Parker, A. D. Ward and A. N. Burgess, *Phys. Rev. Lett.*, 2002, **88**, 246102-246104.
12. R. Aveyard, J. H. Clint, D. Nees and V. N. Paunov, *Langmuir*, 2000, **16**, 1969-1979.
13. D. Frydel, S. Dietrich and M. Oettel, *Phys. Rev. Lett.*, 2007, **99**, 118302.
14. B. J. Park and E. M. Furst, *Soft Matter*, 2011, **7**, 7676-7682.
15. S. Reynaert, P. Moldenaers and J. Vermant, *Langmuir*, 2006, **22**, 4936-4945.
16. C. L. Wirth, E. M. Furst and J. Vermant, *Langmuir*, 2014, **30**, 2670-2675.
17. B. J. Park, J. Vermant and E. M. Furst, *Soft Matter*, 2010, **6**, 5327-5333.
18. W. R. Bowen and A. O. Sharif, *Nature*, 1998, **393**, 663-665.
19. J. J. Gray, B. Chiang and R. T. Bonnecaze, *Nature*, 1999, **402**, 750-750.
20. J. Dobnikar, M. Brunner, H.-H. von Grünberg and C. Bechinger, *Phys. Rev. E*, 2004, **69**, 031402.
21. J. P. Pantina and E. M. Furst, *Langmuir*, 2004, **20**, 3940-3946.
22. B. J. Park and E. M. Furst, *Langmuir*, 2008, **24**, 13383-13392.
23. J. P. Pantina and E. M. Furst, *Phys. Rev. Lett.*, 2005, **94**, 138301-138304.
24. K. C. Neuman and S. M. Block, *Rev. Sci. Instrum.*, 2004, **75**, 2787-2809.
25. J. C. Crocker and D. G. Grier, *J. Colloid Interface Sci.*, 1996, **179**, 298-310.

26. C. A. Schneider, W. S. Rasband and K. W. Eliceiri, *Nat. Meth.*, 2012, **9**, 671-675.
27. B. J. Park and E. M. Furst, *Soft Matter*, 2011, **7**, 7683-7688.
28. A. Ashkin, *Biophys. J.*, 1992, **61**, 569-582.
29. J. D. Feick, N. Chukwumah, A. E. Noel and D. Velegol, *Langmuir*, 2004, **20**, 3090-3095.
30. S. Tan, R. L. Sherman, D. Qin and W. T. Ford, *Langmuir*, 2004, **21**, 43-49.
31. R. M. Simmons, J. T. Finer, S. Chu and J. A. Spudich, *Biophys. J.*, 1996, **70**, 1813.

Table of contents entry

Particle interactions confined in two-dimensional colloidal cages at the oil-water interface are highly pairwise.